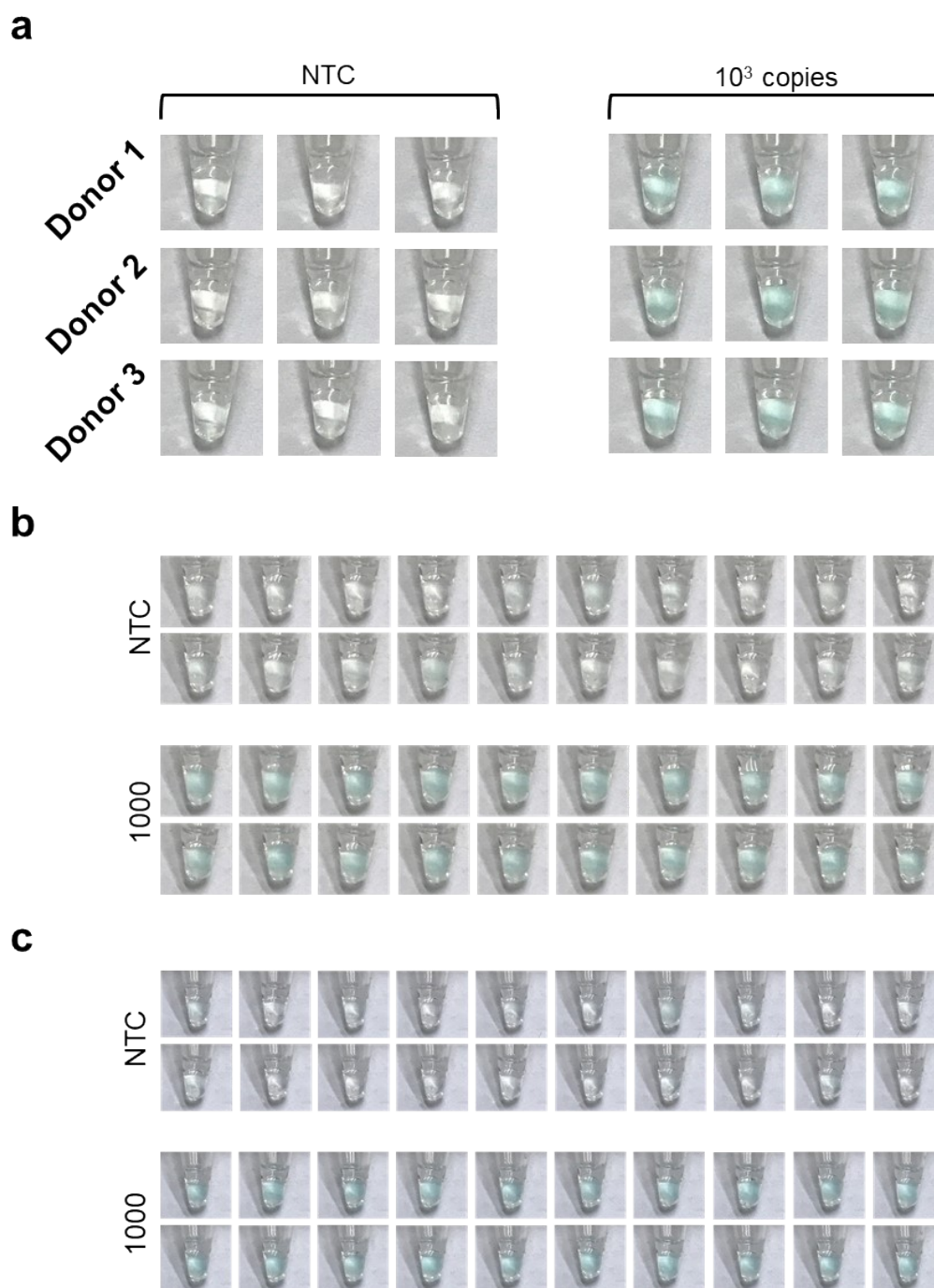
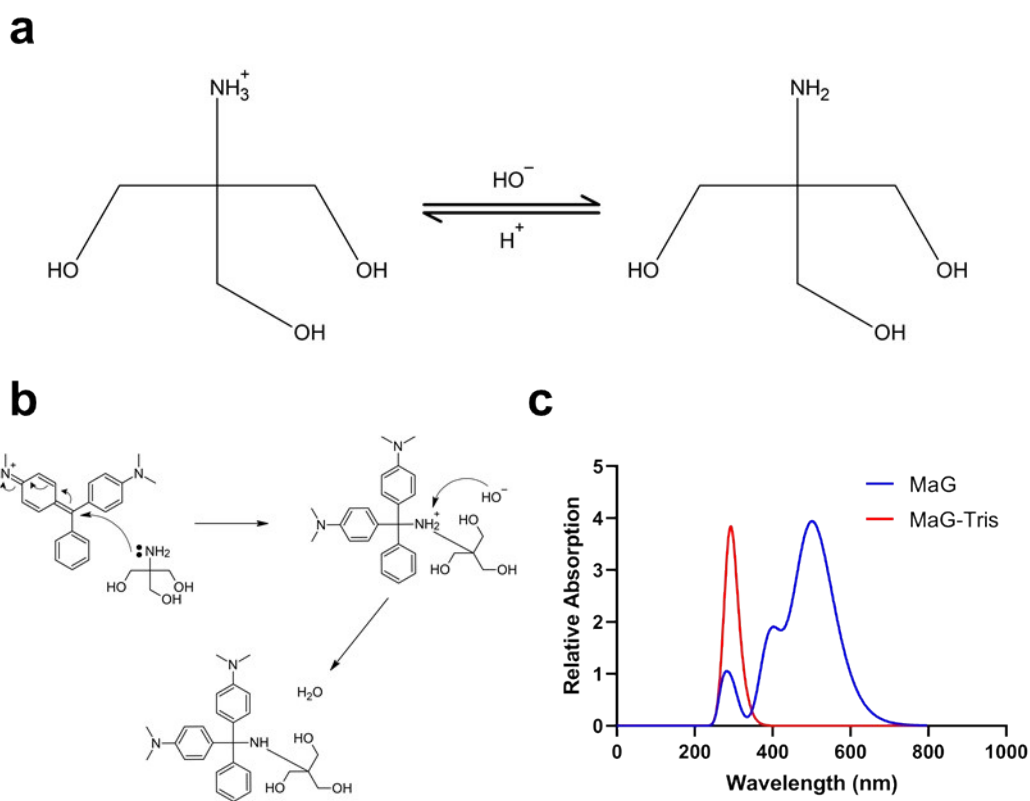


Supplementary Information:

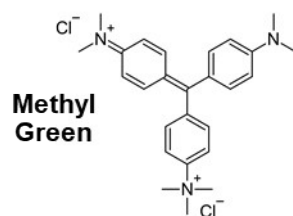
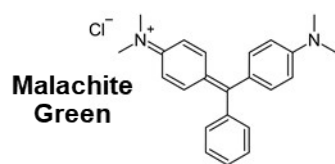
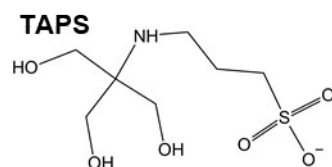
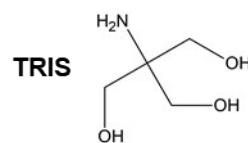
Supplementary Figures:



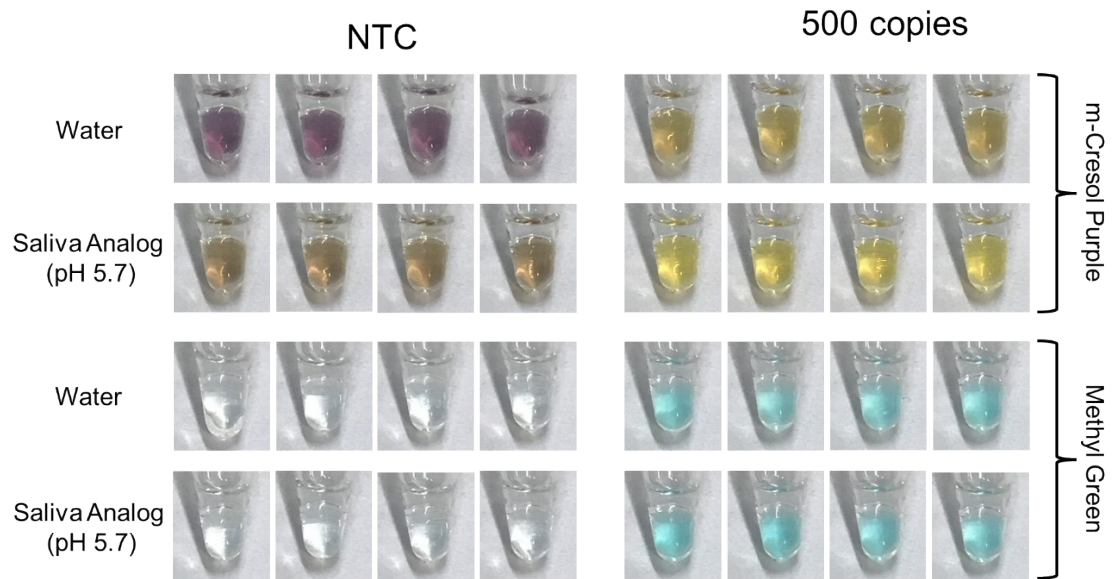
Supplementary Figure 1: RT-LAMP reactions containing heat-treated gargle lavage. (a) Images of RT-LAMP reactions (15 μ L) containing heat-treated gargle lavage (5 μ L) from three donors which were bi-thermally incubated with or without SARS-CoV-2 RNA. Images of RT-LAMP reactions incubated (b) without and (c) with gargle lavage added, with reactions containing either 0 or 1,000 SARS-CoV-2 RNA copies.



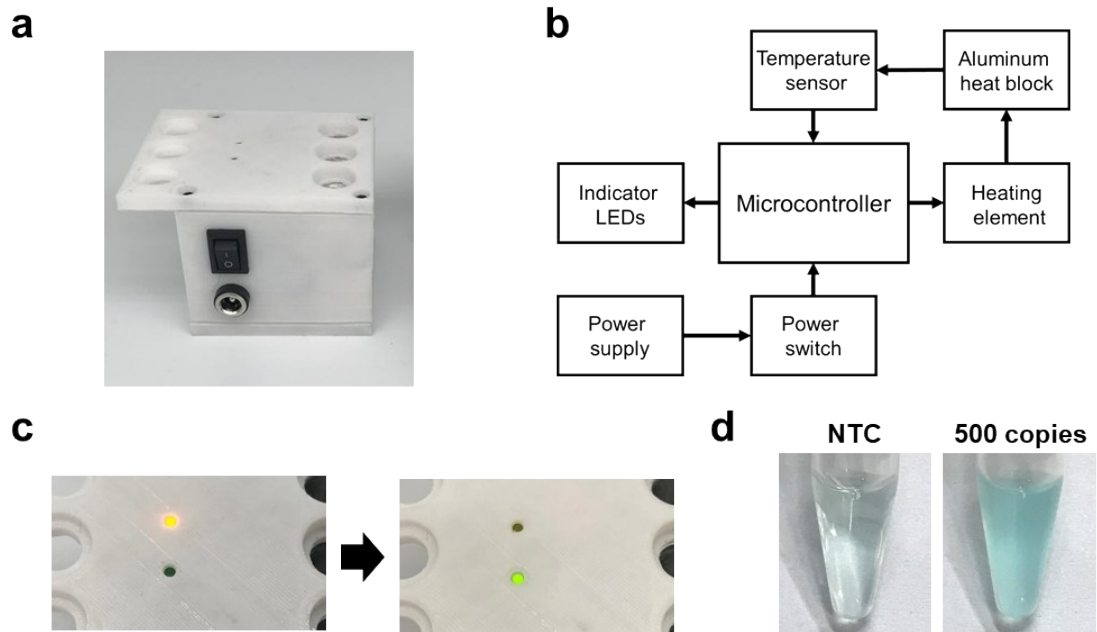
Supplementary Figure 2: Mechanism of Tris-mediated leuco malachite green formation. (a) Dissociation equation for the Tris molecule. (b) Proposed mechanism for formation of tertiary carbinamine during RT-LAMP. (c) Computed UV-Vis spectra of MaG and MaG-Tris tertiary carbinamine.

a**b**

Supplementary Figure 3: Chemical structures. Structures of (a) the triarylmethane dyes malachite green and methyl green and (b) buffer molecules Tris and TAPS.



Supplementary Figure 4: Low pH sample tolerance of halochromic and MeG reactions. Images of RT-LAMP reaction tubes incubated with indicated number of SARS-CoV-2 RNA copies, sample solution (water or saliva analog), and colorimetric dye. All reactions were incubated for 10 minutes at 55°C and 30 minutes at 65°C.



Supplementary Figure 5: Prototype heating device for use in point-of-care diagnostics. (a) The prototype heating device (70 mm L x 55 mm W x 50 mm H) used in this study. (b) Block diagram schematic of the prototype heating device. (c) LEDs are used to indicate when the incubation can begin, switching from yellow to green when the initial target temperature is reached. (d) Images of bi-thermally incubated large-volume RT-LAMP reactions, with 0.002% w/v methyl green and indicated number of SARS-CoV-2 RNA copies.

Orf1a-HMS_F3	CGGTGGACAAATTGTCAC
Orf1a-HMS_B3	CTTCTCTGGATTTAACACACTT
Orf1a-HMS_LF	TTACAAGCTTAAAGAATGTCTGAACACT
Orf1a-HMS_LB	TTGAATTTAGGTGAAACATTTGTCACG
Orf1a-HMSe_FIP	TCAGCACACAAAGCCAAAAATTTATTTTTCTGTGCAAAGG AAATTAAGGAG
Orf1a-HMSe_BIP	TATTGGTGGAGCTAAACTTAAAGCCTTTTCTGTACAATCC CTTTGAGTG

Supplementary Table 1: RT-LAMP primer sequences used in this study.

	Isothermal	Isothermal (40')	Bi-thermal (10' @ 55
--	------------	------------------	----------------------

	(30')		+ 40' @ 65)
NTC	0/20	0/10	0/10
40 copies	3/20 (15%)	5/10 ^{ns} (50%)	8/10 ^{***} (80%)
100 copies	9/10	N/A	N/A

Supplementary Table 2: Isothermal vs bi-thermal incubation in halochromic reactions. (ns = not significant, ***p<0.001, two proportion z-test)

Supplementary Results:

MeG reactions exhibit higher tolerance to low pH samples

A key advantage of triarylmethane dyes is that they can be used for DNA product detection in buffered RT-LAMP reactions, whereas halochromic indicators require minimally buffered reactions¹. This makes halochromic assays inherently susceptible to variability in sample pH and atmospheric intrusion². This disadvantage was illustrated using a buffered saliva analog; the composition and pH of the analog was based on that of resting saliva³⁻⁵, which can be collected for RT-LAMP diagnostics. We observed that a substantial change in color occurred for halochromic reactions, with the color of NTC tubes containing low pH saliva analog being skewed towards that of positive tubes (500 RNA copies) containing water (Supp. Fig. 4). Furthermore, this effect was observed for a sample volume of 3 μ L, which was the largest volume that could be added given that the original halochromic master-mix was 2X. Therefore, the skewed color would presumably be worse with larger sample volumes. In contrast, there was no visually discernible skewing of colors with the buffered MeG reactions (Supp. Fig. 4), highlighting the importance of buffering in RT-LAMP tests, especially given the variability in sample composition that would be encountered by an assay used for testing entire populations.

A prototyped incubation device enables point-of-care use and clear visual readouts

To further address the needs for a COVID-19 home test, a prototype heating device was designed and built to automate the bi-thermal incubation step so that manually changing heat block temperature is not necessary (Supp. Fig. 5a). A casing for the prototype was designed and 3D-printed using acrylonitrile butadiene styrene (ABS) plastic filament. The resulting casing had a glass transition temperature well above the 65 °C used to incubate the reactions and provided suitable insulation between the heat block and user during operation. This casing contained the electronics and heat block (Supp. Fig. 5b). An Arduino Pro Micro microcontroller was programmed to maintain the heat block at 55 °C for 15 minutes, followed by 65 °C for 25 minutes. The initial temperature was reached in approximately three minutes, and it took approximately one minute for the heat block to transition from 55 to 65 degrees. The microcontroller maintained its temperature using a heating pad fixed to the heat block and a temperature sensor mounted inside the heat

block. LED indicators were used to signal when the initial temperature was reached, and an assay could begin (Supp. Fig. 5c). A 0.5 mL tube containing 150 μ L of RT-LAMP reaction solution could then be loaded into the heat block. The larger tube size enabled easier handling and sample loading, and assessment of color change. Using reaction mixtures containing 50 μ L of gargle lavage and 500 copies of SARS-COV-2 RNA for positive reactions (corresponding to 10,000 copies per mL), a distinct color change between negative and positive reactions was observed (Supp. Fig. 5d). The casing for the device also included a small tube rack to enhance user-friendliness. This device could therefore provide a means for home users to test for COVID-19.

Materials and Methods

Oligos

All oligos used in this study were ordered from Tech Dragon (Hong Kong), desalted, and suspended at a concentration of 100 μ M in water. 10 \times LAMP primer master mixes were comprised of 16 μ M FIP, 16 μ M BIP, 2 μ M F3, 2 μ M B3, 4 μ M LF, and 4 μ M LB primers in nuclease-free ultrapure water (Beyotime).

Leuco malachite green assay

Malachite green (SCR chemicals) was mixed at a final concentration of 0.04 % (weight/volume) individually with Tris-HCl solutions at pH 8.8, 7.6, and 6.8 (Beyotime), potassium chloride (Sigma-Aldrich), ammonium sulfate (Sigma-Aldrich), magnesium sulfate (NEB), Tween-20 (BioFroxx), guanidium hydrochloride (Sigma-Aldrich), dNTPs (Beyotime), primers, betaine monohydrate (Sigma-Aldrich), and Bst 2.0 polymerase (NEB) at the stated concentrations. Reactions were incubated at 65°C for 15 minutes, allowed to cool to room temperature for 10 minutes, and imaged.

RT-LAMP assays

Malachite green RT-LAMP reaction mixes contained 1 \times isothermal amplification buffer (NEB), an additional 6 mM MgSO₄, 1.4 mM of each dNTP, 0.04 % w/v malachite green, 1 \times LAMP primer mix, 40 mM guanidine chloride (Sigma-Aldrich), 200 mM betaine monohydrate, 0.3 units/ μ L RTx reverse transcriptase (NEB), and 0.32 units/ μ L Bst 2.0 DNA polymerase. Optimized methyl green reactions contained 1 \times in-house buffer (20 mM Tris-HCl, 10 mM ammonium sulfate, 10 mM potassium chloride, 8 mM magnesium sulfate, .1%

Tween-20, pH 8.8), 1.4 mM of each dNTP, 0.01 % w/v methyl green (Macklin), 1× LAMP primer mix, 200 mM betaine monohydrate, 0.3 units/μL RTx reverse transcriptase (NEB), and 0.32 units/μL Bst 2.0 DNA polymerase. Small reactions were performed in 0.2 mL tubes using 15 μL volumes overlaid with mineral oil (Beyotime), with 1 or 5 μL of sample used in each assay. Large reactions were performed in 0.5 mL tubes using 150 μL volumes and .002% w/v methyl green, with 50 μL of sample used in each assay. Isothermal reactions were incubated at 65 °C for 45 or 60 minutes, while bi-thermal reactions were incubated at 55 °C for 15 minutes followed by 65 °C for 45 minutes. A heat block (Lichen) was used for all 0.2 mL tube reactions. A custom prototyped heating device was used for 0.5 mL reactions.

Minimally buffered colorimetric RT-LAMP reactions contained 1× mCP reaction mix (10 mM ammonium sulfate, 50 mM potassium chloride, 8 mM magnesium sulfate, .1% Tween-20, 100 μM m-cresol purple, pH 8.8), 1.4 mM of each dNTP, 1× LAMP primer mix, 200 mM betaine monohydrate, 0.3 units/μL RTx reverse transcriptase (NEB), and 0.32 units/μL Bst 2.0 DNA polymerase. 15 μL reactions volumes were overlaid with mineral oil in 0.2 mL tubes and incubated at 55°C for 10 minutes and 65°C for 30 minutes.

Control RNA samples

All SARS-COV-2 RNA samples used in this study were derived from the AMPLIRUN SARS-CoV-2 RNA CONTROL (MBC137-R, Vircell). The stock purified RNA concentration was stated as between 1.25×10^4 and 2.00×10^4 copies/μL. For all experiments, we assumed the concentration was 2.00×10^4 copies/μL, to ensure our results were conservative. For simulated gargle lavage samples, 5 mL of sterile water was gargled for 10 seconds and collected in a 15 mL tube. Aliquots were then heat-treated at 95 °C for 30 minutes. Purified RNA samples were then diluted along with heat-treated gargle lavage into RT-LAMP reactions. 10X saliva buffer analog contained 200 mM potassium chloride and 100 mM monosodium phosphate. 1X solutions had their pH adjusted to the desired value with 1M sodium hydroxide.

Cross-contamination prevention

To prevent cross-contamination of RT-LAMP reactions, completed RT-LAMP assay tubes were not opened in the same area where reactions were

prepared. Surfaces were regularly decontaminated with 10 % Clorox bleach solution (~ 1 % hypochlorite).

Image Acquisition, Quantification, and Reaction Outcome Determination

All images were acquired using a smartphone camera (iPhone 7) mounted on a custom 3D-printed support. RT-LAMP assay tubes were cooled to room temperature for 10 minutes after incubation and then photographed under identical lighting conditions and exposure settings. For quantification, a region of interest (ROI) was defined, and images were processed in ImageJ by measuring the ROI's mean saturation. For determining RT-LAMP assay positivity or negativity, k-means clustering in IBM SPSS Statistics software was used to determine a saturation cutoff. For deciding the LOD95 and 95% confidence interval, the probit analysis in IBM SPSS Statistics was used.

Computational UV-Vis Spectra Derivation

All the molecules were optimized by using Kohn-Sham density functional theory (DFT). The hybrid meta-GGA (generalized gradient approach) functional M06-2X combined with the def2SVP basis sets were adopted. Harmonic vibrational analysis was performed to verify all optimized structures are at the local minima. UV-Vis absorption spectra were simulated using the excitation energies and oscillator strengths calculated using the time-dependent DFT (TDDFT) method at the M062X/def2TZVP level. As usual, TDDFT results systematically overestimate the excitation energies of the MaG family^{6,7}. Hence we only focused on the relevant change between relevant compounds as guidance in the spectroscopic assignments. All the computations were performed with the Gaussian 16 program^{8,9}.

Prototype Heating Device

The prototype heating device comprises three main parts: a casing, a microcontroller, and a heat block. The casing consists of 3D-printed acrylonitrile butadiene styrene (ABS) features, designed using FreeCAD (v0.18). The casing encloses the electronics, based around an Arduino Pro Micro microcontroller mounted on an in-house designed (DesignSpark PCB v9.0) printed circuit board (PCB) purchased through JLCPCB. The microcontroller monitors heat block temperature via a single LM35DZ temperature sensor. It uses a proportional-integral-differential PID program (Arduino PID library, v1.2.0) to modulate the current heating pad mounted on the heat block. The heat block is made from a single piece of 6061 aluminum

alloy, with holes machined for holding tubes and the temperature sensor. Indicator LEDs and the electric switch and DC input jack are wired to the microcontroller via the PCB. A 6-volt, 5-amp AC adaptor was used to power the device.

Supplementary References:

1. Tanner, N. A., Zhang, Y. & Evans, T. C. Visual detection of isothermal nucleic acid amplification using pH-sensitive dyes. *Biotechniques* **58**, 59–68 (2015).
2. Dao Thi, V. L. *et al.* A colorimetric RT-LAMP assay and LAMP-sequencing for detecting SARS-CoV-2 RNA in clinical samples. *Sci. Transl. Med.* **12**, eabc7075 (2020).
3. Rehak, N. N., Cecco, S. A. & Csako, G. Biochemical Composition and Electrolyte Balance of 'Unstimulated' Whole Human Saliva *Clin Chem Lab Med* 2000; 38(4):335-343 © 2000 by Walter de Gruyter · Berlin · New York. **38**, 335–343 (2000).
4. Lagerlöf, F. & Oliveby, A. Caries-protective factors in saliva. *Adv. Dent. Res.* **8**, 229–238 (1994).
5. Humphrey & Williamson, R. T. A review of saliva Normal composition, flow, and function. Humphrey, Williamson. 2001. Journal of Prosthetic Dentistry.pdf. *J. Prosthet. Dent.* **85**, 162–169 (2001).
6. Guillaumont, D. & Nakamura, S. Calculation of the absorption wavelength of dyes using time-dependent density-functional theory (TD-DFT). *Dye. Pigment.* **46**, 85–92 (2000).
7. Kawauchi, S., Antonov, L. & Okuno, Y. Prediction of the color of dyes by using time-dependent density functional theory (TD-DFT). *Bulg. Chem. Commun.* **46**, 228–237 (2014).
8. Gaussian 16, Revision A.03, M. J. Frisch, G. W. Trucks, H. B. Schlegel, G. E. Scuseria, M. A. Robb, J. R. Cheeseman, G. Scalmani, V. Barone, G. A. Petersson, H. Nakatsuji, X. Li, M. Caricato, A. V. Marenich, J. Bloino, B. G. Janesko, R. Gomperts, B. Mennu, 2016. Gaussian 16, Revision A.03, M. J. Frisch, G. W. Trucks, H. B. Schlegel, G. E. Scuseria, M. A. Robb, J. R. Cheeseman, G. Scalmani, V. Barone, G. A. Petersson, H. Nakatsuji, X. Li, M. Caricato, A. V. Marenich, J. Bloino, B. G. Janesko, R. Gomperts, B. Mennu.
9. Weigend, F. & Ahlrichs, R. Balanced basis sets of split valence, triple zeta valence and quadruple zeta valence quality for H to Rn: Design and assessment of accuracy. *Phys. Chem. Chem. Phys.* **7**, 3297 (2005).

